

Airway Surface Liquid Volume Regulation Determines Different Airway Phenotypes in Liddle Compared with β ENaC-overexpressing Mice^{*[5]}

Received for publication, June 4, 2010. Published, JBC Papers in Press, June 21, 2010. DOI 10.1074/jbc.M110.151803

Marcus A. Mall^{†§1}, Brian Button[¶], Bjarki Johannesson^{‡§2}, Zhe Zhou[‡], Alessandra Livraghi[¶], Ray A. Caldwell[¶], Susanne C. Schubert[‡], Carsten Schultz^{§||}, Wanda K. O'Neal[¶], Sylvain Pradervand^{**}, Edith Hummler^{**}, Bernard C. Rossier^{**}, Barbara R. Grubb[¶], and Richard C. Boucher[¶]

From the [†]Division of Pediatric Pulmonology and Cystic Fibrosis Center, Department of Pediatrics III, University of Heidelberg, Im Neuenheimer Feld 430, 69120 Heidelberg, Germany, the [§]Molecular Medicine Partnership Unit, University of Heidelberg and European Molecular Biology Laboratory, Im Neuenheimer Feld 350, 69120 Heidelberg, Germany, the ^{||}Cell Biology and Biophysics Unit, European Molecular Biology Laboratory, Meyerhofstrasse 1, 69117 Heidelberg, Germany, the [¶]Cystic Fibrosis/Pulmonary Research and Treatment Center, School of Medicine, University of North Carolina, Chapel Hill, North Carolina 27599-7248, and the ^{**}Department of Pharmacology and Toxicology, University of Lausanne, Bugnon 27, CH-1005 Lausanne, Switzerland

Studies in cystic fibrosis patients and mice overexpressing the epithelial Na⁺ channel β -subunit (β ENaC-Tg) suggest that raised airway Na⁺ transport and airway surface liquid (ASL) depletion are central to the pathogenesis of cystic fibrosis lung disease. However, patients or mice with Liddle gain-of-function β ENaC mutations exhibit hypertension but no lung disease. To investigate this apparent paradox, we compared the airway phenotype (nasal *versus* tracheal) of Liddle with CFTR-null, β ENaC-Tg, and double mutant mice. In mouse nasal epithelium, the region that functionally mimics human airways, high levels of CFTR expression inhibited Liddle epithelial Na⁺ channel (ENaC) hyperfunction. Conversely, in mouse trachea, low levels of CFTR failed to suppress Liddle ENaC hyperfunction. Indeed, Na⁺ transport measured in Ussing chambers ("flooded" conditions) was raised in both Liddle and β ENaC-Tg mice. Because enhanced Na⁺ transport did not correlate with lung disease in these mutant mice, measurements in tracheal cultures under physiologic "thin film" conditions and *in vivo* were performed. Regulation of ASL volume and ENaC-mediated Na⁺ absorption were intact in Liddle but defective in β ENaC-Tg mice. We conclude that the capacity to regulate Na⁺ transport and ASL volume, not absolute Na⁺ transport rates in Ussing chambers, is the key physiologic function protecting airways from dehydration-induced lung disease.

The amiloride-sensitive epithelial Na⁺ channel (ENaC)³ is a heteromultimeric protein composed of three subunits (α , β , and γ). ENaC is limiting for the absorption of salt and water from airway and other epithelia, including renal and colonic epithelia (1–3). Increased ENaC-mediated airway Na⁺ absorption is a hallmark of cystic fibrosis (CF) (4, 5), a genetic form of chronic obstructive lung disease caused by mutations in the cystic fibrosis transmembrane conductance regulator (CFTR) gene (6, 7). Numerous studies have indicated that CFTR functions as a Cl[−] channel regulated by cAMP-dependent phosphorylation and as a regulator of ENaC in airway epithelia (1, 8–11). Previous *in vitro* studies indicated that the increased Na⁺ absorption in CF airways is caused by increased apical membrane ENaC activity, reflecting deficient inhibition by mutant CFTR, and that Na⁺ hyperabsorption is associated with airway surface liquid (ASL) volume depletion and impaired mucus clearance (12–14).

The concept that increased airway Na⁺ absorption and ASL volume depletion play a critical role in the *in vivo* pathogenesis of CF lung disease, however, remains controversial. For example, a recent hypothesis proposes that an acidic ASL pH, due to deficient HCO₃[−] secretion by mutant CFTR, rather than deficient ASL volume regulation, produces increased mucus viscosity, reduced mucus clearance, and CF airway disease (15). The role of ASL volume depletion in CF pathogenesis was buttressed by a recently developed mouse model with airway-specific overexpression of β ENaC under the control of the Clara cell secretory protein promoter (16). In this mouse model, selective airway overexpression of β ENaC was sufficient to increase airway Na⁺ absorption, cause ASL volume depletion,

* This work was supported, in whole or in part, by National Institutes of Health Grants SCOR P50 HL60280 and P01 HL 34322 (to R. C. B.). This work was also supported by Deutsche Forschungsgemeinschaft Grants DFG MA 2081/3-2, MA 2081/3-3, and MA 2081/4-1 (to M. A. M.) and European Commission Grant MEXT-CT-2004-013666 (to M. A. M.).

[5] The on-line version of this article (available at <http://www.jbc.org>) contains supplemental Figs. 1–4.

¹ To whom correspondence should be addressed: Division of Pediatric Pulmonology and Cystic Fibrosis Center, Dept. of Pediatrics III, University of Heidelberg, Im Neuenheimer Feld 430, 69120 Heidelberg, Germany. Tel.: 49-6221-568840; Fax: 49-6221-568806; E-mail: Marcus.Mall@med.uni-heidelberg.de.

² Supported by an EMBL Ph.D. fellowship.

³ The abbreviations used are: ENaC, epithelial sodium channel; ASL, airway surface liquid; CFTR, cystic fibrosis transmembrane conductance regulator; CF, cystic fibrosis; L/L, mice homozygous for the Liddle mutation; CF mice, mice that are deficient in CFTR; CF-Liddle mice, CF mice homozygous for the Liddle mutation; β ENaC-Tg, mice overexpressing the epithelial Na⁺ channel β -subunit; PD, potential difference; I_{sc} , short circuit current; I_{eq} , equivalent short circuit current; I_{amil} , amiloride-sensitive I_{eq} ; I_{max} , maximal amiloride-sensitive I_{eq} ; I_{frct} , fractional HA ENaC population; R_{te} , transepithelial resistance.

ENaC and ASL Regulation

reduce mucus clearance, and produce a spontaneous lung disease that shared key features with CF and other chronic obstructive pulmonary diseases, including substantial pulmonary mortality, airway mucus obstruction, goblet cell metaplasia, chronic airway inflammation, and slowed clearance of bacterial pathogens (16, 17). Taken together, the results from these *in vitro* and *in vivo* studies suggest that increased airway Na⁺ absorption, produced either by deficient CFTR-mediated inhibition of ENaC in human CF airways or by transgenic overexpression of wild-type βENaC in murine airways, causes ASL volume depletion, which initiates a series of pathogenetic steps that cause chronic obstructive lung disease.

Importantly, a third mechanism exists that can increase epithelial Na⁺ absorption. Gain-of-function mutations have been identified in the genes encoding β- and γENaC (*Scnn1b* and *Scnn1g*) that cause a constitutive increase in Na⁺ transport in the distal nephron of the kidney, resulting in an autosomal dominant form of salt-sensitive hypertension known as Liddle syndrome or pseudoaldosteronism (18–20). The molecular pathogenesis of Liddle syndrome has been studied in detail, and it has been demonstrated that the disease is caused by mutations that delete a proline-rich (PY) motif in the C termini of β- and γENaC that is critical for binding of the ubiquitin-protein ligase Nedd4-2. Nedd4-2 binding leads to ubiquitination and retrieval of ENaC from the plasma membrane. In Liddle syndrome, abrogation of the ENaC/Nedd4-2 interaction results in an increased number of ENaC channels in the plasma membrane, producing increased renal sodium absorption and salt sensitive hypertension (21–23). Because Nedd4-2 binding to ENaC is under control of Sgk1 (serum- and glucocorticoid-induced kinase 1), both Nedd4-2 and Sgk1 are key regulators of ENaC in the kidney (24–26).

Little is known about the pulmonary phenotype in Liddle syndrome, but Liddle patients do not develop overt lung disease (27, 28). In a mouse model that carries the classical Liddle mutation (*i.e.* a premature stop codon in the *Scnn1b* gene corresponding to the R556X mutation in Liddle patients), it has been shown that this gain-of-function mutation causes increased Na⁺ absorption in the distal nephron of the kidney, the colon, and the alveolar air spaces of the lung, but the phenotype of the conducting airways has not been studied (29–33). The aim of the present study was to elucidate the effects of this endogenously expressed gain-of-function mutation in βENaC on airway Na⁺ and volume transport and correlate each parameter with phenotypes in the upper (nasal) and lower airways. Studies of the lower airways included (i) Ussing chamber measurements of transepithelial Na⁺ transport under “flooded” conditions in native tissues, (ii) confocal ASL volume measurements under physiologic “thin film” conditions in cultured preparations, and (iii) a morphologic search for evidence of abnormal regulation of Na⁺ transport *in vivo*.

EXPERIMENTAL PROCEDURES

Experimental Animals—All animal studies were approved by the animal care and use committee of the University of North Carolina at Chapel Hill and the Regierungspräsidium Karlsruhe, Germany. The generation and genotyping of Liddle mice, βENaC-Tg mice, and CF (*Cftr*^{-/-}) mice has been

described previously (16, 29, 34, 35). Liddle mice were originally generated on a mixed genetic background (129Ola × C57BL/6J) and were backcrossed for >5 generations to the C57BL/6J background. βENaC-Tg mice (line 6608) were generated on a mixed genetic background (C3H/HeN × C57BL/6N) and were backcrossed (N10) to the C57BL/6J background. CF mice were on a mixed genetic background (BALB/c, C57BL/6, DBA/2, and 129/SvEv). Mice heterozygous for the Liddle mutation (L/+) were interbred, and homozygous Liddle mice (L/L) and wild-type (WT) littermates were studied at the age of 12–16 weeks. CF mice were intercrossed with Liddle mice and double mutant CF mice homozygous for the Liddle mutation (CF-Liddle), and CF, L/L, and WT littermate controls were studied at the age of 16–54 weeks. βENaC-Tg mice and WT littermates were 6–8 weeks of age. Airway epithelial necrosis was studied in 3-day-old mice of respective genotypes. Mice were housed in specific pathogen-free animal facilities. CF mice received Colyte instead of drinking water to prevent intestinal obstruction. All other animals had free access to regular chow and water.

In Vivo Potential Difference (PD) Measurements—For *in vivo* studies of transepithelial PD, mice were anesthetized via intraperitoneal injection of avertin (0.4 g/kg tribromoethanol, 0.4 ml/kg amyl alcohol), and the body temperature was continually monitored with a rectal thermocouple (Physitemp) and maintained at 37 °C with a heat lamp. Nasal and rectal PD measurements were performed, and the basal PD and the amiloride-sensitive PD were determined as described previously (29, 36).

Ussing Chamber Measurements—Mice were killed with 100% CO₂, nasal and tracheal tissues were removed and mounted on modified Ussing chambers, and bioelectric measurements were taken as described previously (13, 16, 37). In most studies, we used recirculating chambers to measure basal short circuit current (*I*_{sc}) and the sequential effects of amiloride (100 μmol/liter; luminal), forskolin (10 μmol/liter; luminal), and UTP (100 μmol/liter; luminal). Studies on protease regulation of ENaC-mediated Na⁺ transport and amiloride dose-response studies were performed in continuously perfused chambers under open circuit conditions, and the equivalent short circuit current (*I*_{eq}) was calculated from the PD and the transepithelial resistance (*R*_{te}) according to Ohm's law (*i.e.* *I*_{eq} = PD/*R*_{te}) as described previously (13). Dose-response curves were obtained by measuring the change in *I*_{eq} induced by exposing tissues to increasing concentrations of amiloride (10⁻⁹ to 10⁻³ mol/liter) and plotted as remaining amiloride-sensitive *I*_{eq} (*I*_{amil}) normalized to the maximal amiloride-sensitive *I*_{eq} (*I*_{max}). IC₅₀ values were determined by fitting dose-response data to the Hill equation with the Hill coefficient constrained to 1.0 as follows,

$$I_{\text{amil}} = I_{\text{max}} \times (1 - 1/(1 + IC_{50}/A)) \quad (\text{Eq. 1})$$

where *A* is the apical bath amiloride concentration. Additionally, data were fitted with a two-component Hill model,

$$I_{\text{amil}} = I_{\text{max}} \times (1 - I_{\text{frct}}/(1 + IC_{50\text{HA}}/A) + (1 - I_{\text{frct}})/(1 + IC_{50\text{LA}}/A)) \quad (\text{Eq. 2})$$

where subscripts HA and LA denote the high affinity and low affinity IC₅₀, respectively, and *I*_{frct} is the fractional HA ENaC

population. The LA ENaC population = $1 - I_{\text{frct}}$. The models that best fit the dose-response data were judged based on comparison of S.E. using an F-test distribution,

$$F_{\text{calc}}(k_1, n - k_2) = (S_1 - S_2) \times (n_1 - k_2) / (S_2 \times k_2) \quad (\text{Eq. 3})$$

where S is the residual sum of squares, n is the number of data points, k is the number of free parameters, and subscripts 1 and 2 depict parameters of the one- and two-component Hill model, respectively (38). For studies of ENaC regulation by extracellular serine proteases, tissues were equilibrated in the presence of the protease inhibitor aprotinin (100 $\mu\text{g}/\text{ml}$, ~ 3.8 trypsin inhibitory units/mg; Sigma) added to the apical bath, and the effect of amiloride (100 $\mu\text{mol}/\text{liter}$; luminal) was either measured in the presence of aprotinin alone or after adding a ~ 2 -fold excess of trypsin (550 $\mu\text{g}/\text{ml}$, $\sim 14,000$ *N*-benzoyl-L-arginine ethyl ester units/mg; Sigma) on the basis of activity (1 trypsin unit = 9000 *N*-benzoyl-L-arginine ethyl ester units).

Real-time RT-PCR—Mice were killed with 100% CO_2 and nasal and tracheal tissues were immediately removed and stored in RNAlater (Ambion, Austin, TX). Total RNA was isolated using the RNeasy kit (Qiagen Inc., Valencia, CA) and reverse transcribed into cDNA using Superscript II (Invitrogen). Quantification of αENaC , βENaC , γENaC , CFTR, Nedd4-2, and Sgk1 mRNA expression was performed using SYBR Green detection in a LightCycler PCR machine according to the manufacturer's instructions (Roche Applied Science) and the following custom made primers (MWG Biotech, High Point, NC): αENaC , 5'-CGG AGT TGC TAA ACT CAA CATC-3' (sense) and 5'-TGG AGA CCA GTA CCG GCT-3' (antisense); βENaC , 5'-TAA TGG AGG CAG TCC TGG-3' (sense) and 5'-GTT GGC AGA AGG AAG TGT CT-3' (antisense); γENaC , 5'-CAG GCG CAT AGC AGA GGT A-3' (sense) and 5'-ACC TGG CCA AGC TCT TGA TA-3' (antisense); CFTR, 5'-ACC ACA GGC ATA ATC ATG G-3' (sense) and 5'-AGC AGA ATG AAA CTC TTC CAC-3' (antisense); Nedd4-2, 5'-GAT ACC CTT TCC AAT CCA CA-3' (sense) and 5'-AGG ACG TCA GGT CTC TTT ACA-3' (antisense); Sgk1, 5'-ACA ACA TCT ACC TTC TGT GGC-3' (sense) and 5'-CAT AAA GTC ATC CTT GGC AC-3' (antisense). Relative -fold changes in target gene expression were calculated from the efficiency of the PCR and the crossing point deviation between samples from experimental groups and determined by normalization to expression of the reference gene 18 S or β -actin, as described previously (17).

Histology and Airway Morphometry—Adult mice were killed with 100% CO_2 , and neonatal mice were killed by decapitation. Lungs were removed through a median sternotomy, immersion-fixed in 4% buffered formalin, and embedded in paraffin. Sections were cut at 5 μm and stained with hematoxylin and eosin (H&E) or Alcian blue periodic acid-Schiff as described previously (16). Necrotic airway epithelial cells were identified by morphologic criteria (*i.e.* cell swelling with cytoplasmic vacuolization), and numeric cell densities were quantitated by counting epithelial cells/mm of the basement membrane as described previously (17).

Primary Tracheal Epithelial Cultures—Mice were euthanized with 100% CO_2 , the tracheas were removed, and epithe-

lial cells were isolated and cultured on membranes (T-Col, Costar, Cambridge, MA) under air-liquid interface conditions and studied after reaching confluence (10 days), and some cultures were subjected to Ussing chamber studies to determine amiloride-sensitive Na^+ transport, as described previously (16).

ASL Height Measurements—Primary tracheal epithelial cultures were washed, and 20 μl of PBS containing 0.2% (v/v) Texas Red-dextran (10 kDa; Molecular Probes) was added to the lumen to visualize the ASL layer. Adding this volume of PBS results in an initial ASL height of ~ 20 – 30 μm , as described previously (39). Images of the Texas Red-labeled ASL were acquired by laser-scanning confocal microscopy (LSM 510, Carl Zeiss, Jena, Germany) using the appropriate filters for Texas Red (540 nm excitation/630 nm emission). To avoid evaporation of the thin ASL layer, 100 μl of immiscible perfluorocarbon (Fluorinert-77, 3M Corp.) was added to the airway surface following the addition of the labeling dye (39). The height of the ASL was measured by averaging the heights obtained from xz scans of five predetermined points on the culture. In the experiments described here, ASL height was measured 15 min following the addition of the Texas Red-dextran and at designated time points over a period of 24 h in primary tracheal epithelial cultures from Liddle mice, βENaC -Tg mice, and their respective WT littermates.

Statistics—All data were analyzed with SigmaStat version 3.1 (Systat Software, Erkrath, Germany) and are reported as mean \pm S.E. Statistical analyses were performed using Student's *t* test, the Mann-Whitney rank sum test, one-way analysis of variance, and Kruskal-Wallis analysis of variance on ranks as appropriate, and $p < 0.05$ was accepted to indicate statistical significance.

RESULTS

The Liddle Mutation Does Not Cause Gain of Na^+ Transport Function in Nasal Epithelia—To study the effect of the Liddle mutation on airway Na^+ transport, we first performed *in vivo* measurements of nasal PD in Liddle mice and WT littermate controls. Basal and amiloride-sensitive nasal PD values in WT mice were similar to those in previous studies (36), and neither value was different in Liddle mice (Fig. 1A). In contrast, rectal PD measurements demonstrated that both basal and amiloride-sensitive rectal PD were significantly increased in Liddle mice compared with WT controls (supplemental Fig. 1), as described previously (29). The absence of increased Na^+ absorption in nasal epithelia of Liddle mice was confirmed by *in vitro* measurements of basal and amiloride-sensitive transepithelial short circuit current (I_{sc}) across freshly excised nasal epithelia (Fig. 1B). Furthermore, following amiloride pretreatment, cAMP-stimulated Cl^- secretion was the same in Liddle and WT tissues (supplemental Fig. 2A). Ca^{2+} -activated (UTP) Cl^- secretion was absent in both genotypes (supplemental Fig. 2A), as described previously for WT mice (36).

The Liddle Mutation Does Cause Gain of Na^+ Transport Function in Tracheal Epithelia—Because previous studies from CF mice suggested that the regulation of ENaC function differs in mouse upper and lower airways (36, 37, 40), we also studied the effect of the Liddle mutation on ion transport in freshly

ENaC and ASL Regulation

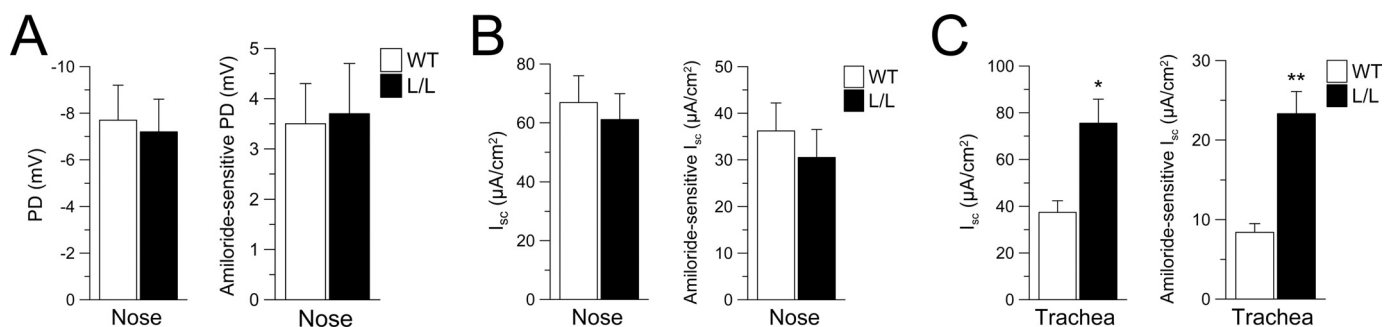


FIGURE 1. **Effect of the Liddle mutation on airway Na^+ absorption.** A–C, *in vivo* measurements of basal and amiloride-sensitive nasal PD (A) and *ex vivo* measurements of basal and amiloride-sensitive I_{sc} in nasal tissues (B) and tracheal tissues (C) from Liddle (L/L) and WT mice. $n = 5$ –17 mice/group. *, $p < 0.05$; **, $p < 0.001$ compared with WT. Error bars, S.E.

excised tracheal epithelia. The magnitude of amiloride-sensitive Na^+ absorption in WT mice was substantially smaller in tracheal than nasal epithelia (Fig. 1, B and C). However, basal and amiloride-sensitive I_{sc} were significantly increased in tracheal tissues from Liddle compared with WT tracheas (Fig. 1C). Following amiloride pretreatment, the magnitude of Cl^- secretion stimulated by either cAMP or Ca^{2+} agonists did not differ between Liddle and WT mice (supplemental Fig. 2B). This indicates that agonist-mediated Cl^- secretory capacity was not altered by the Liddle mutation under conditions of amiloride block.

Expression of ENaC Subunits and ENaC Regulators in Upper and Lower Airway Epithelia—To identify mechanisms regulating Na^+ transport rates in nasal *versus* tracheal epithelia in WT and Liddle mice, we measured transcript levels of individual α -, β -, and γ ENaC subunits and several known ENaC regulators, including CFTR, the ubiquitin protein ligase Nedd4-2, and the serum and glucocorticoid-activated kinase Sgk1 in freshly excised tissues from both genotypes (10, 11, 23, 24, 26).

To investigate the differences in Na^+ transport rates in WT *versus* Liddle mouse airways, transcript levels in Liddle mice were normalized to levels in WT mice. Expression of the mutated β ENaC was significantly reduced in both Liddle nasal and tracheal tissues, as described previously for kidney and colon, probably reflecting RNA instability caused by the residual loxP site in the targeting construct (29) (Fig. 2). However, expression levels of α ENaC, γ ENaC, Nedd4-2, Sgk1, and CFTR were not different in Liddle mice compared with WT controls in either nasal or tracheal epithelia (Fig. 2, A and B).

To determine the differences in nasal *versus* tracheal Na^+ transport, we normalized transcript levels in nasal to tracheal epithelia of WT mice. Consistent with higher Na^+ transport in nasal *versus* tracheal epithelia (Fig. 1, B and C), these studies revealed that expression levels of α -, β -, and γ ENaC were all significantly increased in the nose compared with the trachea (Fig. 2C). Although Nedd4-2 and Sgk1 were also relatively increased in nasal epithelia, the highest -fold change in expression was for CFTR mRNA, which was ~ 20 -fold higher in nasal compared with tracheal epithelia (Fig. 2C).

CFTR Inhibits Gain of ENaC Function in Nasal Epithelia from Liddle Mice—To more directly investigate the role of CFTR in regulation of the Liddle mutated ENaC in native airway tissues, we generated double mutant mice that were deficient in CFTR (CF) and homozygous for either the Liddle muta-

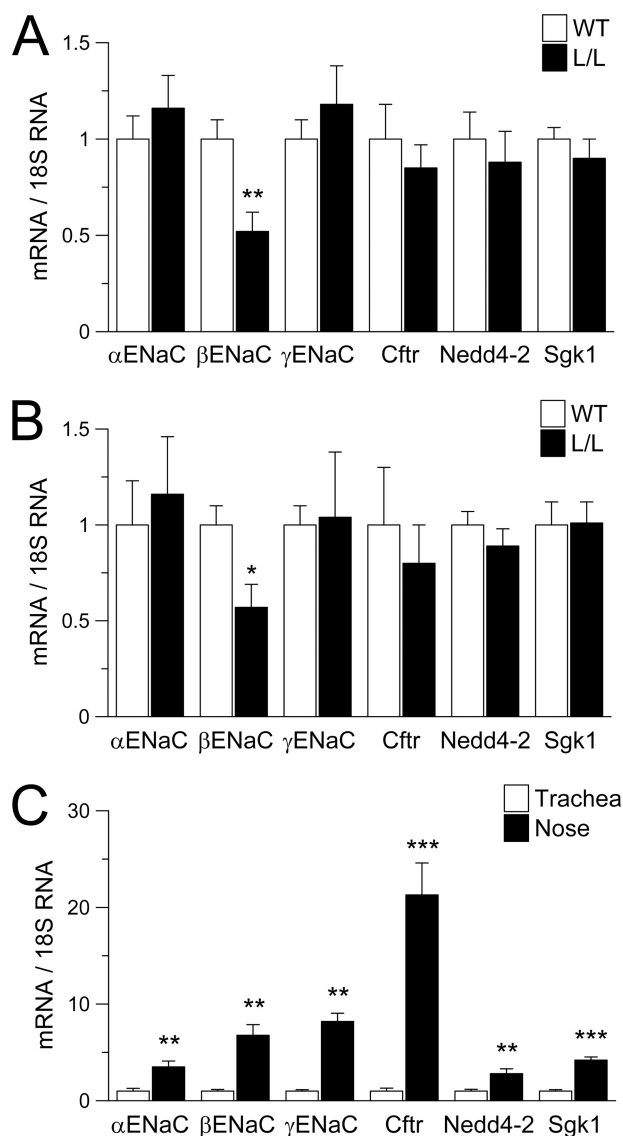


FIGURE 2. **Expression of ENaC subunits and ENaC regulators in nasal and tracheal epithelia.** A–C, transcript levels of α ENaC, β ENaC, γ ENaC, CFTR, Nedd4-2, and Sgk1 in freshly excised nasal and tracheal tissues from L/L and WT mice. A and B, comparison of transcript expression levels in nasal (A) and tracheal (B) tissues from L/L *versus* WT mice. Data are expressed as -fold changes from WT. $n = 5$ –6 mice/group; *, $p < 0.05$; **, $p < 0.01$. C, comparison of expression levels in tracheal tissues (open bars) *versus* nasal tissues (closed bars) from WT mice. Data are expressed as -fold changes from tracheal tissues. $n = 5$ –6 mice/group; **, $p < 0.01$; ***, $p < 0.001$. Error bars, S.E.

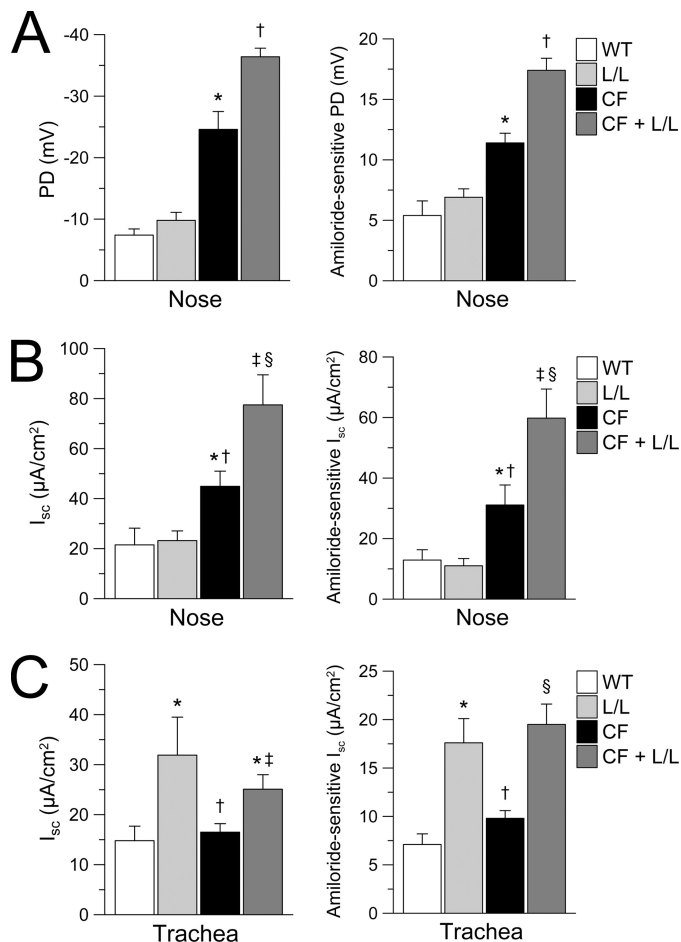


FIGURE 3. Effect of the Liddle mutation on airway Na⁺ absorption in CFTR-deficient mice. A–C, *in vivo* measurements of basal and amiloride-sensitive nasal PD (A) and *ex vivo* measurements of basal and amiloride-sensitive I_{sc} in nasal tissues (B) and tracheal tissues (C) from WT mice, L/L mice, single mutant CFTR-deficient (CF) mice, and double mutant CFTR-deficient Liddle (CF + L/L) mice. A, nasal PD measurements. *n* = 8–12 mice/group. *, *p* < 0.001 compared with WT and L/L mice; †, *p* < 0.001 compared with WT, L/L, and CF mice. B, nasal I_{sc} measurements. *n* = 5–7 mice/group. *, *p* < 0.05 compared with WT and L/L mice; †, *p* < 0.02 compared with L/L mice; ‡, *p* < 0.01 compared with WT and L/L mice; §, *p* < 0.05 compared with CF mice. C, tracheal I_{sc} measurements. *n* = 6–9 mice/group. *, *p* < 0.05 compared with WT mice; †, *p* < 0.01 compared with L/L mice; ‡, *p* ≤ 0.02 compared with CF mice; §, *p* < 0.001 compared with WT and CF mice. Error bars, S.E.

tion (CF-Liddle) or the wild-type *Scnn1b* allele and performed *in vivo* nasal PD measurements and transepithelial Ussing chamber measurements on nasal and tracheal epithelia (Fig. 3, A–C). *In vivo* nasal PD measurements demonstrated that basal and amiloride-sensitive PD were significantly increased in double mutant CF-Liddle, in a stepwise relationship, compared with (i) the raised PDs of CF littermates, (ii) “normal” PDs of Liddle mice with a wild-type CFTR genotype, and (iii) WT mice (Fig. 3A). Further, *in vitro* measurements of transepithelial I_{sc} revealed similar stepwise relationships for basal and amiloride-sensitive I_{sc} in nasal tissues from CF-Liddle compared with CF mice, Liddle mice expressing wild-type CFTR, or WT mice (Fig. 3B). Conversely, in tracheal tissues, the lack of CFTR had no effect on basal and amiloride-sensitive I_{sc} in CF-Liddle compared with Liddle mice (Fig. 3C). Similar to Liddle mice expressing wild-type CFTR (supplemental Fig. 2), Cl[−] secretory capacity following activation with forskolin or UTP was not different in amiloride-pretreated nasal or tracheal tissues from CF-Liddle mice compared with CF controls (supplemental Fig. 3). Taken together, these data indicate that wild-type CFTR inhibits the Liddle ENaC gain of Na⁺ transport function when both proteins are co-expressed in the nasal epithelium. Conversely, these data are consistent with the hypothesis that low levels of tracheal CFTR expression were insufficient to inhibit the Liddle ENaC gain of function in the trachea.

Morphologic Evaluation of Lungs from Liddle Mice—Liddle mice exhibited normal survival and no spontaneous airway disease phenotype, including absence of histological evidence of mucus obstruction, goblet cell metaplasia, or airway inflammation, compared with WT controls (Fig. 4). Similar to the findings in Liddle mice, airways pathology was also absent in double mutant CF-Liddle mice (Fig. 4). In contrast, βENaC-Tg mice with a comparable level of increased tracheal Na⁺ absorption at 4–8 weeks after birth exhibit airway mucus plugging, airway epithelial remodeling with goblet cell hyperplasia, neutrophilic inflammation, and emphysema (16, 17).

ASL Volume Regulation by WT, Liddle, and βENaC-Tg Cultured Airway Epithelia—Airway epithelial volume homeostasis requires the capacity to reciprocally regulate Na⁺ absorption and Cl[−] secretion (39, 41). Our previous studies demonstrated that airway Na⁺ hyperabsorption induced by tissue-specific

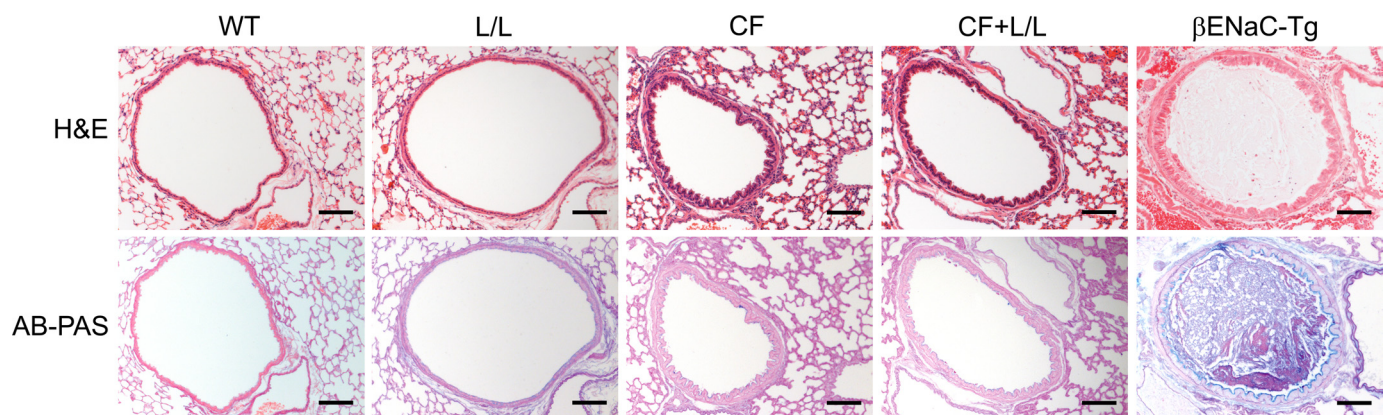


FIGURE 4. Effect of the Liddle mutation on airway morphology. Lung histology from adult WT mice, L/L mice, CF mice, double mutant CFTR-deficient Liddle (CF + L/L) mice, and βENaC-Tg mice stained with H&E and Alcian blue periodic acid-Schiff (AB-PAS). Scale bars, 100 μm. Results shown are representative for *n* = 6–14 mice/group.

ENaC and ASL Regulation

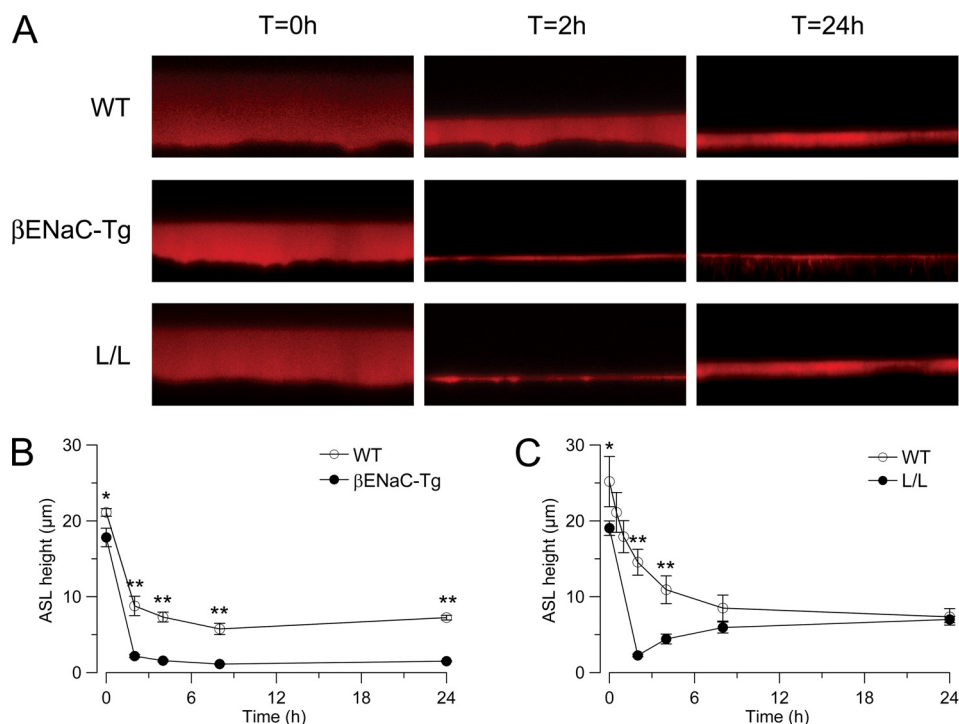


FIGURE 5. ASL volume regulation in airway epithelia from Liddle mice and β ENaC-Tg mice. A–C, Confocal images (A) and summary of measurements of ASL height (B and C) at 0, 2, 4, 8, and 24 h after the mucosal addition of 20 μ l of PBS containing Texas Red dextran to primary tracheal epithelial cultures from β ENaC-Tg (A and B), L/L mice (A and C), and the respective WT littermates. Scale bars, 7 μ m. $n = 3$ –6 mice/group. *, $p < 0.05$ compared with WT. **, $p < 0.01$ compared with WT. Error bars, S.E.

overexpression of β ENaC causes ASL volume depletion and deficient mucus clearance *in vivo*, indicating that overexpression of β ENaC produced an unregulated ENaC channel that produced lung disease via airway surface dehydration (16, 17). To test the hypothesis that the absence of pulmonary pathology in Liddle mice reflected “normal” regulation of Liddle ENaC *in vivo* in the lung, we generated the primary epithelial culture preparations required for studies of ASL volume regulation under physiologic thin film conditions. Similar to freshly excised tracheal tissues, Ussing chamber studies under flooded conditions demonstrated that amiloride-sensitive Na^+ transport was significantly increased in tracheal cultures from Liddle mice ($\Delta I_{sc} = 21.8 \pm 5.4 \mu\text{A}/\text{cm}^2$, $n = 12$ for WT; $\Delta I_{sc} = 60.7 \pm 15.3 \mu\text{A}/\text{cm}^2$, $n = 12$ for Liddle; $p < 0.05$) and β ENaC-Tg mice ($\Delta I_{sc} = 13.9 \pm 3.4 \mu\text{A}/\text{cm}^2$, $n = 6$ for WT; $\Delta I_{sc} = 45.9 \pm 7.9 \mu\text{A}/\text{cm}^2$, $n = 5$ for β ENaC-Tg; $p < 0.01$) compared with WT controls.

For ASL measurements under thin film conditions, a small volume of liquid (20 μ l) was added to the luminal compartment of confluent tracheal cultures grown at an air-liquid interface, and ASL height was monitored sequentially over a period of 24 h by confocal laser-scanning microscopy (39, 41). In WT cultures, the added liquid was largely absorbed within a period of ~ 4 h. Subsequently, ASL height was maintained at $\sim 6 \mu\text{m}$, corresponding to the height of extended cilia in mice (Fig. 5). This volume homeostatic response probably reflected the inhibition of Na^+ transport and acceleration of Cl^- secretion reported during ASL volume homeostasis in cultured normal human airway epithelia (39, 41). In cultures from β ENaC-Tg mice, the initial rate of liquid ab-

sorption was significantly increased compared with WT controls, consistent with increased Na^+ absorption. Importantly, these cultures failed to slow absorption when ASL approached the height of outstretched cilia and removed all of the available liquid from airway surfaces (Fig. 5A). This pattern of ASL volume hyperabsorption reflects increased and unregulated airway Na^+ absorption, a pattern also observed in human CF airway cultures (14, 39). In tracheal cultures from Liddle mice, similar to β ENaC-Tg mice, initial ASL volume absorption was also accelerated, and ASL was almost entirely removed from culture surfaces within 2 h following the volume challenge. However, in contrast to β ENaC-Tg cultures, where ASL remained depleted, Liddle epithelia added ASL to their surfaces during the 7–24 h phase and regulated ASL height to levels similar to WT controls (*i.e.* $\sim 6 \mu\text{m}$) (Fig. 5B).

The Liddle Mutation Does Not Cause Airway Epithelial Cell Necrosis—The confocal ASL data suggest that Liddle ENaC is regulated in the lower airways at physiologic ASL volumes, whereas β ENaC-Tg channels are not. To search for *in vivo* correlates of Na^+ channel regulation, we quantitated the number of Clara cells undergoing hydropic degeneration. Hydropic degeneration has been reported in neurons in *Caenorhabditis elegans* that express gain-of-function mutations in a channel homologous to ENaC, the degenerin channel (42, 43). The gain-of-function mutations in the degenerin channel appear to lock the channel into an unregulated open mode with an open probability (P_o) approaching 1.0. Necrotic (hydropic degenerated) cells were detected in airway epithelia from neonatal β ENaC-Tg mice (Fig. 6, A and B) but not in adult β ENaC-Tg mice (data not shown), as reported previously (17). In contrast to β ENaC-Tg mice, we detected no necrotic cells in airways of Liddle mice at any time period (Fig. 6, A and B).

ENaC Sensitivity to Amiloride in Airways of WT, Liddle, and β ENaC-Tg Mice—The presence of necrotic cells in the airway epithelium of β ENaC-Tg mice, but not Liddle mice, suggested a defect in ENaC regulation in β ENaC-Tg but not Liddle murine airway epithelia. We therefore searched for a mechanism that may predict abnormal regulation of β ENaC-Tg channels. In the β ENaC-Tg mice, β ENaC is expressed >20 –100-fold greater than the endogenous β ENaC, raising the possibility that $\alpha\beta$ ENaC channels, heterologous expression of α - and β ENaC subunits in *Xenopus* oocytes produces reduced whole cell Na^+ currents, probably due to inefficient processing of $\alpha\beta$ ENaC (1). However, $\alpha\beta$ ENaC channels that are inserted into the plasma

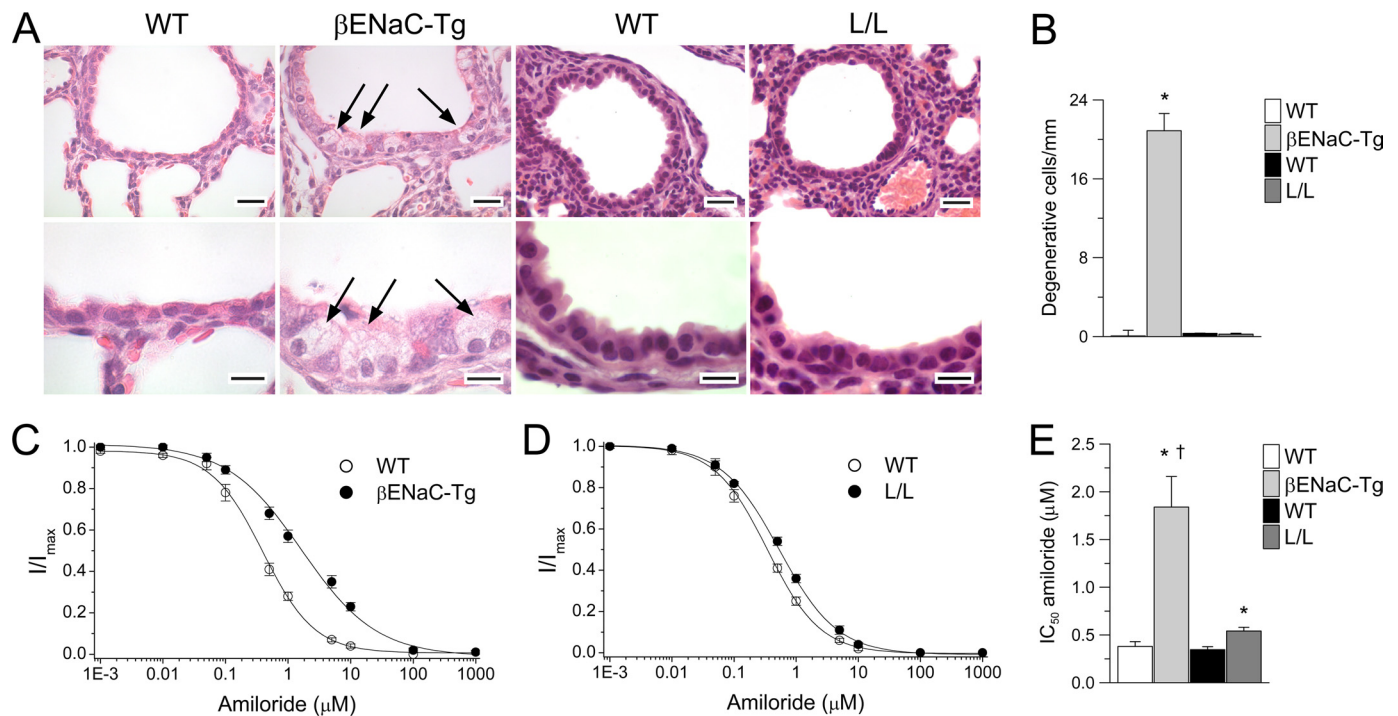


FIGURE 6. Regulation of ENaC in airway epithelia is abnormal in β ENaC-Tg mice but preserved in Liddle mice. *A*, airway histology from neonatal (3-day-old) β ENaC-Tg mice, L/L mice, and their respective WT littermates. Sections were stained with H&E and evaluated for degenerative airway epithelial cells (arrows). Scale bars, 20 μ m (upper panels) and 10 μ m (lower panels). *B*, summary of airway epithelial necrosis as determined from the number of degenerative epithelial cells per mm of the basement membrane. $n = 3-5$ mice for each group. *, $p \leq 0.01$ compared with WT. *C-E*, amiloride dose-response curves (*C* and *D*) and summary of IC_{50} values (*E*) obtained from tracheal tissues of β ENaC-Tg mice, L/L mice, and respective WT littermates. $n = 6-12$ mice/group. *, $p < 0.01$ compared with WT mice; †, $p = 0.001$ compared with L/L mice. Error bars, S.E.

TABLE 1

Hill model dose-response fit parameters \pm S.E. for ENaC channels in native tracheal epithelia of WT, L/L, and β ENaC-Tg mice

Parameters were obtained from averaged amiloride dose-response data (see Fig. 6, *C* and *D*) fitted with single and two-component Hill equations (see "Experimental Procedures"). Results are consistent with tracheal tissues from β ENaC-Tg mice expressing a subpopulation of ENaC channels with low affinity toward amiloride. NS, not significantly different.

	Single component Hill model IC_{50}	Two-component Hill model			Statistical comparison single versus two-component model ^a
		High affinity IC_{50}	High affinity relative population I_{fract}	Low affinity IC_{50}	
	μ M	μ M	%	μ M	
WT	0.3 ± 0.0	0.3 ± 0.2	86 ± 105	0.9 ± 4.4	NS
L/L	0.6 ± 0.0	0.2 ± 0.2	22 ± 31	0.8 ± 0.3	NS
β ENaC-Tg	1.8 ± 0.4	0.6 ± 0.1	64 ± 3.2	30.9 ± 0.7	$p < 0.025$

^a β ENaC-Tg $F_{calc}(3, 7) = 59.3$; WT $F_{calc}(3, 5) = 0.2$; Liddle $F_{calc}(3, 5) = 2.5$.

membrane have a resting open probability of ~ 1.0 , compared with ~ 0.5 for heterologously expressed $\alpha\beta\gamma$ ENaC channels (44). This finding suggests that $\alpha\beta$ ENaC channels are abnormally regulated in oocytes so that they are maximally activated under resting conditions. Another important characteristic of the $\alpha\beta$ ENaC channel is that it is less sensitive to amiloride than the $\alpha\beta\gamma$ ENaC channel in oocytes, with the amiloride IC_{50} shifted about 1 log to the right of $\alpha\beta\gamma$ ENaC (1, 11, 45). In contrast to alveolar epithelial cells (46), it was not possible to obtain cell-attached membrane patches from the apical membrane of well differentiated mouse airway epithelial cells to measure P_o directly. We therefore tested the hypothesis that β ENaC-Tg may express abnormally regulated $\alpha\beta$ ENaC channels by characterizing the amiloride sensitivity of freshly excised tracheas from β ENaC-Tg, Liddle, and WT mice.

Analysis of amiloride dose-response curves using a single component Hill model demonstrated that the amiloride IC_{50} for Liddle tracheas was slightly shifted (~ 1.5 -fold) to the right

of WT littermate controls. However, in β ENaC-Tg tracheas, the shift in IC_{50} to the right of WT tissues was significantly larger (~ 4.8 -fold), suggesting that the sensitivity to amiloride was significantly reduced in β ENaC-Tg compared with Liddle tracheas (Fig. 6, *C-E*). Modeling of dose-response curves with a single component versus a two-component Hill model demonstrated that the amiloride dose-response curve in β ENaC-Tg tracheas was described significantly better by the two-component model compared with the single component model ($p < 0.025$). This finding is consistent with two channel populations (*i.e.* a high affinity channel population ($IC_{50} = 0.6 \pm 0.1$ μ mol/liter) and a second population of low affinity channels ($IC_{50} = 30.9 \pm 10.7$ μ mol/liter)), which constituted $\sim 35\%$ of the total ENaC channel population (Table 1). In contrast, IC_{50} values determined by the single component versus the two-component Hill model did not differ statistically in WT and Liddle tracheas (Table 1), consistent with expression of a single high affinity ENaC channel population in WT and Liddle mice.

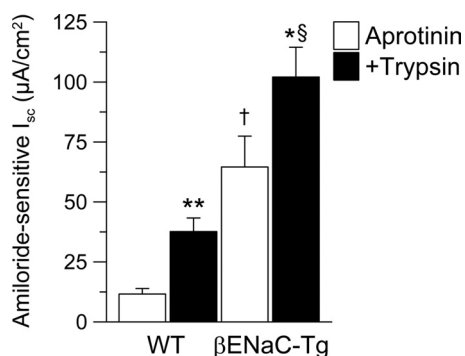


FIGURE 7. Regulation of ENaC by extracellular proteases is abnormal in airway epithelia from β ENaC-Tg mice. Freshly excised tracheal tissues from WT and β ENaC-Tg mice were pretreated with luminal aprotinin, and amiloride-sensitive I_{sc} was measured either in the presence of aprotinin alone (Aprotinin) or after the addition of luminal trypsin (+Trypsin). $n = 9-14$ mice/group. *, $p < 0.05$; **, $p < 0.001$ compared with mice of same genotype; †, $p < 0.001$ compared with WT mice; §, $p < 0.001$ compared with β ENaC-Tg mice. Error bars, S.E.

Thus, these data suggest that the necrotic cells in β ENaC-Tg mouse airways may reflect excessive Na^+ absorption via a population of unregulated $\alpha\beta$ ENaC channels, whereas the absence of necrotic cells suggests that the Liddle $\alpha\beta\gamma$ ENaC channel is sufficiently regulated *in vivo* to protect airway epithelia from necrosis.

ENaC Regulation by Extracellular Proteases Is Abnormal in Airways of β ENaC-Tg Mice—Recent studies demonstrated that proteolytic activation of $\alpha\beta\gamma$ ENaC channels by extracellular serine proteases plays an important role in regulating ENaC-mediated Na^+ absorption in airway epithelia. However, protease-dependent activation is not required for $\alpha\beta$ ENaC channels, suggesting that the γ ENaC subunit is essential in this process (47–49). To further test the hypothesis that β ENaC-Tg mice express abnormally regulated $\alpha\beta$ ENaC channels, we compared ENaC regulation by both block of protease activation (aprotinin) and application of trypsin as a prototypic serine protease in freshly excised WT and β ENaC-Tg tracheal tissues. To maximize the effect of the block of protease activation of ENaC, these experiments were performed in the presence of the serine protease inhibitor aprotinin from the time immediately after tracheal excision to a measure of steady state current 30 min after mounting of the tissues in Ussing chambers. Amiloride-sensitive Na^+ transport was measured both under steady state (aprotinin) conditions and after the addition of luminal trypsin. Under steady state aprotinin conditions, the amiloride-sensitive I_{sc} was significantly (~ 5.5 -fold) increased in trachea from β ENaC-Tg compared with WT mice (Fig. 7). The subsequent addition of trypsin to the luminal bath increased the amiloride-sensitive I_{sc} by a similar magnitude in WT and β ENaC-Tg tracheae ($\Delta I_{sc} = 26.0 \pm 5.6 \mu\text{A}/\text{cm}^2$, $n = 10$ for WT; $\Delta I_{sc} = 37.5 \pm 12.4 \mu\text{A}/\text{cm}^2$, $n = 14$ for β ENaC-Tg; $p < 0.93$), reducing the ratio of amiloride-sensitive I_{sc} in β ENaC *versus* WT mice to ~ 2.7 -fold, typical for β ENaC-Tg and WT tissues in the absence of aprotinin (16). Taken together, these data indicate that WT and β ENaC-Tg airway epithelia express a similar number of apical membrane $\alpha\beta\gamma$ ENaC channels that are largely inhibited by aprotinin and reactivated by trypsin. The β ENaC-Tg mice express a population of $\alpha\beta$ channels that are not regulated by

proteases, accounting for the proportionately reduced effects of aprotinin and trypsin in β ENaC-Tg mice as compared with WT mice.

DISCUSSION

Proper regulation of ASL volume, a function dependent on coordinate regulation of ENaC-mediated Na^+ absorption and CFTR/CaCC-mediated Cl^- secretion, plays a critical role in maintaining the normal mucociliary clearance component of lung defense (50, 51). Therefore, defects in either process (*i.e.* active Cl^- secretion or Na^+ absorption) are predicted to produce ASL depletion, mucociliary dysfunction, and lung disease. The aim of this study was to elucidate the role of abnormal ENaC function and ASL volume regulation in the *in vivo* pathogenesis of chronic airway disease. We therefore studied a mouse model of a gain-of-function mutation in ENaC (Liddle) reported to exhibit increased Na^+ absorption in renal and colonic epithelia (29–32). Our investigations led us to study both (i) why Liddle-mediated increased Na^+ transport was expressed in the tracheal but not nasal epithelium and (ii) why, despite Ussing chamber measured increases in Na^+ transport in the Liddle trachea, there was no associated lung disease.

First, we sought the mechanisms to explain the apparent discordance of the Liddle Na^+ transport phenotype in the two respiratory regions (Fig. 1). The expression of all three ENaC subunits (α , β , and γ) is required to obtain maximal Na^+ currents (1), and CFTR, Nedd4-2, and Sgk1 have been reported to regulate apical membrane ENaC number and activity (10, 12, 23–26). We therefore hypothesized that absence of increased Na^+ absorption in nasal epithelia from Liddle compared with WT mice was caused by reduced expression of α - or γ ENaC subunits or increased expression of ENaC regulators in nasal epithelia from Liddle compared with WT mice. Comparison of ENaC subunit expression levels between WT and Liddle mice confirmed a $\sim 50\%$ reduction in Liddle β ENaC transcripts in nasal epithelia, as previously described for kidney and colon (29). However, no differences in expression levels of α - or γ ENaC or other ENaC regulators between WT and Liddle nasal tissues were detected that could compensate for the Liddle gain-of-function mutation (Fig. 2).

However, we noted that the level of CFTR expression in mice was markedly higher in nasal compared with tracheal epithelia in both WT and Liddle mice (Fig. 2). The importance of CFTR in regulation of Na^+ transport rates in mice has been suggested previously by observations from CF mice. In CF mice, the amiloride-sensitive I_{sc} is raised in the nasal epithelia, but not trachea, reflecting the likelihood that CFTR is expressed at levels sufficient to regulate ENaC in the nasal cavity but that other regulatory paths dominate in the lower airways, where CFTR expression is very low (36, 37, 40). The role of CFTR in regulation of Liddle ENaC in native airway tissues has not been studied, and co-expression studies in heterologous cells produced conflicting results. Whereas one study suggested that CFTR inhibits ENaC channels carrying Liddle mutations, including stop mutations that produce truncations of the C termini of β - and γ ENaC (52), another study indicated that C termini of β -

and γ ENaC are required for functional interaction between CFTR and ENaC (53).

To genetically study the role of CFTR in regulation of Liddle ENaC in native nasal *versus* tracheal epithelia, we crossed CF mice with Liddle mice and observed a \sim 2-fold increase in PD in CF-Liddle nasal as compared with CF nasal epithelia. The additivity in rates of Na^+ transport observed in the CF-Liddle mice compared with CF mice is consistent with the absence of CFTR-mediated inhibition of ENaC in CF mice (10, 11, 13) and gain of ENaC function in the Liddle mice (21, 54). In contrast, the rates of Na^+ transport in CF-Liddle and Liddle tracheas were not different (Fig. 3), consistent with the relative absence of CFTR expression, and hence CFTR regulatory function, in either the Liddle or WT tracheas.

Thus, these genetic and functional studies demonstrate that CFTR plays a critical role in the regulation of both WT and Liddle ENaC in nasal epithelial cells that co-express ENaC and CFTR. Similar to Liddle patients expressing the R556X mutation, the C terminus of the β ENaC subunit is truncated in Liddle mice. Therefore, our studies suggest that the functional interaction between CFTR and ENaC in native nasal tissues did not rely on the presence of the β ENaC C terminus. The gain of Na^+ transport function in the tracheas of Liddle mice is consistent with data reporting Liddle mediated gain of Na^+ transport function in other epithelia in which CFTR is expressed at low levels (e.g. the cortical collecting duct of the kidney or the surface epithelium of the colon) (3, 55). Because in humans, unlike mice, CFTR is co-expressed with ENaC at relatively high levels in the surface epithelium of both upper and lower airways (56), our findings also may explain why patients with Liddle syndrome do not develop CF-like lung disease (27, 28).

Second, we investigated why increased Na^+ absorption in the lower airways of Liddle mice did not cause CF-like lung disease. In contrast to β ENaC-Tg mice, Liddle mice exhibited an absence of airway mucus obstruction, goblet cell hyperplasia, or inflammation (Fig. 4) (29, 33). We hypothesized that it may not be an increase in the absolute rate of Na^+ transport but rather the lack of regulation of Na^+ transport required for normal ASL volume homeostasis that caused lung disease.

We tested the hypothesis that β ENaC-Tg mice cannot regulate ENaC sufficiently for ASL volume homeostasis *in vitro*, whereas Liddle mice can, by measuring ASL homeostasis in primary tracheal cultures under thin film conditions in response to a volume challenge. Normal mouse airway epithelia exhibited ASL volume regulation similar to human epithelia, with a key feature being inhibition of ENaC-mediated Na^+ transport as excess liquid is absorbed from the airway surface (Fig. 5). The volume response of β ENaC-Tg tracheal cultures was strikingly similar to the response observed in human CF airway cultures (i.e. initially accelerated absorption, failure to slow absorption at low ASL volume, and steady state depletion of ASL volume from epithelial surfaces) (Fig. 5) (39, 41). This physiology is consistent with a failure to regulate (inhibit) ENaC at low ASL volumes.

In tracheal cultures from Liddle mice, consistent with increased Na^+ absorption observed in Ussing chamber experiments under flooded conditions, the rate of absorption of the added liquid was accelerated. However, in con-

trast to β ENaC-Tg epithelia, “normal” ASL volume homeostasis was achieved in \sim 6 h by Liddle tracheal cultures following the removal of excess fluid, and ASL remained at a steady state thereafter. With respect to the delay of normal homeostatic ASL regulation in Liddle compared with WT mice, we speculate that Liddle (and WT) ENaC may be regulated by soluble inhibitor(s) that were diluted after the volume challenge and reconcentrated under thin film conditions. For example, previous studies demonstrated that ENaC is activated by proteolytic cleavage and blocked by protease inhibitors, suggesting that an endogenous protease/antiprotease system plays an important role in CFTR-independent regulation of ENaC on airway surfaces (49, 57–59). Further, recent evidence suggested that ENaC-activating proteases are membrane-anchored, whereas protease inhibitors are soluble and can therefore act as ASL sensors to inhibit ENaC activity under thin film conditions (60). Because the Liddle mutation results in an increased number of active ENaC channels on the plasma membrane, we speculate that (i) the early rapid phase of volume absorption reflected the activity of a relatively (to WT) large number of active ENaC channels on the membrane, and (ii) the return to normal ASL homeostatic volumes reflected the gradual accumulation of potentially higher concentrations of inhibitor required to prevent activation of Liddle channels newly inserted into the plasma membrane. Thus, “normal” ASL regulation under steady state conditions in Liddle epithelia suggests the preservation of regulation (inhibition) of Liddle ENaC under thin film conditions (Fig. 5).

A finding consistent with the key role of Na^+ transport (ENaC) inhibition in ASL regulation in β ENaC-Tg *versus* Liddle mice *in vitro* was observed *in vivo* (i.e. necrotic cells were detected in neonatal β ENaC-Tg but not in Liddle mouse airways). Like degenerin mutation-expressing neurons in *C. elegans* (42, 43), the presence of necrotic cells suggests unregulated entry of Na^+ into β ENaC-Tg-expressing Clara cells, leading to hydropic degeneration and necrosis. In a previous study, we demonstrated that hydropic degeneration in neonatal β ENaC-Tg airways was reduced by preventive treatment with amiloride (61). Interestingly, a link between Na^+ channel dysregulation and cell death was also established in an animal model for Duchenne muscular dystrophy. In *mdx* mice, the absence of dystrophin causes dysregulation of the skeletal muscle isoforms of the voltage-gated Na^+ channel $\text{Na}_v1.4$, producing intracellular Na^+ overload and cell death, which were both prevented by a specific $\text{Na}_v1.4$ blocker (62). Taken together, these data indicate that degeneration and cell death were a direct consequence of dysregulated airway Na^+ absorption in β ENaC-Tg mice. In contrast, necrotic cells were not detected in neonatal Liddle airway epithelia, suggesting that there was sufficient regulation of Liddle ENaC channels *in vivo* to prevent this event (Fig. 6).

Of note, hydropic degeneration was only observed in neonatal and not in adult β ENaC-Tg airways (17). We speculate that several factors may explain why Clara cells in adult β ENaC-Tg mice were protected from degeneration and cell death. Previous studies demonstrated that the activity of the Clara cell secretory protein promoter peaks in newborn mice and wanes thereafter (63). Consistent with this finding, Clara cell secretory

protein-driven induction of β ENaC transcripts and amiloride-sensitive I_{sc} was significantly greater in neonatal compared with adult β ENaC-Tg mice (supplemental Fig. 4). These results suggest that lower levels of Na^+ hyperabsorption may protect Clara cells in adult β ENaC-Tg airways from undergoing hydropic degeneration. Additionally, Clara cells may be more susceptible to Na^+ influx in the neonatal period. For example, in contrast to adult airways, Clara cells in neonatal airways store large amounts of glycogen, which were depleted by Na^+ hyperabsorption in β ENaC-Tg mice, suggesting that differences in energy metabolism in neonatal *versus* adult Clara cells may contribute to susceptibility to cell death (17). Further, our previous studies demonstrated that mucus plugging of central airways is more severe in neonatal *versus* adult β ENaC-Tg mice. Therefore, airway hypoxia resulting from severe airway mucus plugging may also contribute to cell death triggered by Na^+ hyperabsorption in neonatal β ENaC-Tg airways (17).

We hypothesized that the failure to regulate Na^+ transport in mice overexpressing the β ENaC subunit (β ENaC-Tg) reflected the expression of a population of protease activation-independent $\alpha\beta$ ENaC channels in the luminal membrane of airway epithelial cells. Indeed, we detected evidence for $\alpha\beta$ ENaC channels, as reflected in the relative insensitivity of Na^+ transport to amiloride inhibition and the detection of a subpopulation of low affinity ENaC channels in native tracheal tissues from β ENaC-Tg mice (Fig. 6 and Table 1) (44). Further, our data suggest that tracheal epithelia from β ENaC-Tg mice express a pool of $\alpha\beta$ ENaC channels that remained constitutively active during aprotinin treatment and were not activated by subsequent trypsin addition (Fig. 7). Taken together with previous studies demonstrating that (i) proteolytic cleavage by extracellular proteases regulates ENaC activity by increasing its P_o and (ii) that the γ ENaC subunit plays an essential role in this process (47–49), our results are consistent with the hypothesis that airways from β ENaC-Tg mice express $\alpha\beta$ ENaC channels that exhibit a basal P_o of ~ 1.0 (44) and are insensitive to normal inhibitors of ENaC activity, including endogenous protease inhibitors (59, 60) present in ASL *in vitro* and in the vicinity of necrotic cells *in vivo*.

An important hypothesis generated by our comparisons of Na^+ transport in Ussing chambers *versus* thin film conditions with the development of lung disease in Liddle *versus* β ENaC-Tg mice is that it is the regulation of Na^+ transport, not the maximal rate of Na^+ transport, that determines whether airway surfaces are adequately hydrated for health. This hypothesis is consistent with recent data that suggest that bypassing the normal regulation of ENaC at low ASL volumes with an unregulated “exogenous channel” (e.g. nystatin) can produce a phenotype of ASL depletion and mucus adhesion to airway surfaces (64). In the mouse experiments described here and in human bronchial epithelial cells treated with mucosal nystatin (64), the persistence of the capacity to secrete Cl^- is not sufficient to protect the hydration status of the airway surface. This result probably reflects the inability of airway epithelia to generate driving forces sufficient to secrete Cl^- in the absence of ENaC inhibition (65).

In summary, our study demonstrated that CFTR inhibits the increase in Na^+ absorption caused by Liddle ENaC when the

two proteins are endogenously co-expressed in nasal epithelia. Because humans also co-express both CFTR and ENaC in the lower airways, we suggest that this mechanism protects Liddle patients from CF-like lung disease (28, 56). Importantly, our studies in mice indicate that, under physiological thin film conditions, non-CFTR-mediated regulatory factors inhibit the raised Na^+ absorption intrinsic to the Liddle mutation in ENaC and thus mediate normal ASL homeostasis and protect Liddle mice from lower airway disease. The importance of ASL volume regulation was buttressed by the observation that transgenic overexpression of wild-type β ENaC escaped the ENaC regulation required for ASL homeostasis and produced airway dehydration and CF-like lung disease. Further elucidation of the pathways that regulate ENaC under thin film conditions may produce novel therapeutic targets for pulmonary diseases caused by increased ENaC-mediated Na^+ absorption, such as CF.

Acknowledgments—We gratefully acknowledge the expert technical assistance of Kim Burns, Elizabeth Hudson, Stephanie Hirtz, Jolanthe Schatterny, and Troy Rogers. We thank Dr. Beverly Koller for providing CF mice.

REFERENCES

- Canessa, C. M., Schild, L., Buell, G., Thorens, B., Gautschi, I., Horisberger, J. D., and Rossier, B. C. (1994) *Nature* **367**, 463–467
- Rossier, B. C., Pradervand, S., Schild, L., and Hummler, E. (2002) *Annu. Rev. Physiol.* **64**, 877–897
- Kunzelmann, K., and Mall, M. (2002) *Physiol. Rev.* **82**, 245–289
- Knowles, M. R., Stutts, M. J., Spock, A., Fischer, N., Gatzky, J. T., and Boucher, R. C. (1983) *Science* **221**, 1067–1070
- Boucher, R. C., Stutts, M. J., Knowles, M. R., Cantley, L., and Gatzky, J. T. (1986) *J. Clin. Invest.* **78**, 1245–1252
- Kerem, B., Rommens, J. M., Buchanan, J. A., Markiewicz, D., Cox, T. K., Chakravarti, A., Buchwald, M., and Tsui, L. C. (1989) *Science* **245**, 1073–1080
- Welsh, M. J., Ramsey, B. W., Accurso, F., and Cutting, G. R. (2001) in *The Metabolic and Molecular Bases of Inherited Disease* (Scriver, C. R., Beaudet, A. L., Sly, W. S., and Valle, D., eds) pp. 5121–5188, McGraw-Hill, New York
- Anderson, M. P., Gregory, R. J., Thompson, S., Souza, D. W., Paul, S., Mulligan, R. C., Smith, A. E., and Welsh, M. J. (1991) *Science* **253**, 202–205
- Sheppard, D. N., and Welsh, M. J. (1999) *Physiol. Rev.* **79**, S23–S45
- Stutts, M. J., Canessa, C. M., Olsen, J. C., Hamrick, M., Cohn, J. A., Rossier, B. C., and Boucher, R. C. (1995) *Science* **269**, 847–850
- Mall, M., Hipper, A., Greger, R., and Kunzelmann, K. (1996) *FEBS Lett.* **381**, 47–52
- Willumsen, N. J., and Boucher, R. C. (1991) *Am. J. Physiol.* **261**, C332–C341
- Mall, M., Bleich, M., Greger, R., Schreiber, R., and Kunzelmann, K. (1998) *J. Clin. Invest.* **102**, 15–21
- Matsui, H., Grubb, B. R., Tarran, R., Randell, S. H., Gatzky, J. T., Davis, C. W., and Boucher, R. C. (1998) *Cell* **95**, 1005–1015
- Quinton, P. M. (2008) *Lancet* **372**, 415–417
- Mall, M., Grubb, B. R., Harkema, J. R., O’Neal, W. K., and Boucher, R. C. (2004) *Nat. Med.* **10**, 487–493
- Mall, M. A., Harkema, J. R., Trojanek, J. B., Treis, D., Livraghi, A., Schubert, S., Zhou, Z., Kreda, S. M., Tilley, S. L., Hudson, E. J., O’Neal, W. K., and Boucher, R. C. (2008) *Am. J. Respir. Crit. Care Med.* **177**, 730–742
- Liddle, G. W., Bledsoe, T., and Coppage, W. S. (1963) *Trans. Assoc. Am. Physicians* **76**, 199–213
- Shimkets, R. A., Warnock, D. G., Bositis, C. M., Nelson-Williams, C., Hansson, J. H., Schambelan, M., Gill, J. R., Jr., Ulick, S., Milora, R. V., and

- Findling, J. W. (1994) *Cell* **79**, 407–414
20. Hansson, J. H., Nelson-Williams, C., Suzuki, H., Schild, L., Shimkets, R., Lu, Y., Canessa, C., Iwasaki, T., Rossier, B., and Lifton, R. P. (1995) *Nat. Genet.* **11**, 76–82
 21. Snyder, P. M., Price, M. P., McDonald, F. J., Adams, C. M., Volk, K. A., Zeiher, B. G., Stokes, J. B., and Welsh, M. J. (1995) *Cell* **83**, 969–978
 22. Abriel, H., Loffing, J., Rebhun, J. F., Pratt, J. H., Schild, L., Horisberger, J. D., Rotin, D., and Staub, O. (1999) *J. Clin. Invest.* **103**, 667–673
 23. Kamynina, E., Debonneville, C., Bens, M., Vandewalle, A., and Staub, O. (2001) *FASEB J.* **15**, 204–214
 24. Chen, S. Y., Bhargava, A., Mastroberardino, L., Meijer, O. C., Wang, J., Buse, P., Firestone, G. L., Verrey, F., and Pearce, D. (1999) *Proc. Natl. Acad. Sci. U.S.A.* **96**, 2514–2519
 25. Debonneville, C., Flores, S. Y., Kamynina, E., Plant, P. J., Tauxe, C., Thomas, M. A., Münster, C., Chraïbi, A., Pratt, J. H., Horisberger, J. D., Pearce, D., Loffing, J., and Staub, O. (2001) *EMBO J.* **20**, 7052–7059
 26. Kamynina, E., and Staub, O. (2002) *Am. J. Physiol. Renal Physiol.* **283**, F377–F387
 27. Baker, E., Jeunemaitre, X., Portal, A. J., Grimbert, P., Markandu, N., Persu, A., Corvol, P., and MacGregor, G. (1998) *J. Clin. Invest.* **102**, 10–14
 28. Stutts, M. J., Homolya, V., Robinson, J., Zhou, J., Boucher, R. C., and Knowles, M. R. (1998) *Ped. Pulmonol.* **217**, Suppl. 17 (abstract)
 29. Pradervand, S., Wang, Q., Burnier, M., Beermann, F., Horisberger, J. D., Hummler, E., and Rossier, B. C. (1999) *J. Am. Soc. Nephrol.* **10**, 2527–2533
 30. Dahlmann, A., Pradervand, S., Hummler, E., Rossier, B. C., Frindt, G., and Palmer, L. G. (2003) *Am. J. Physiol. Renal Physiol.* **285**, F310–F318
 31. Pradervand, S., Vandewalle, A., Bens, M., Gautschi, I., Loffing, J., Hummler, E., Schild, L., and Rossier, B. C. (2003) *J. Am. Soc. Nephrol.* **14**, 2219–2228
 32. Bertog, M., Cuffe, J. E., Pradervand, S., Hummler, E., Hartner, A., Porst, M., Hilgers, K. F., Rossier, B. C., and Korbmacher, C. (2008) *J. Physiol.* **586**, 459–475
 33. Randrianarison, N., Escoubet, B., Ferreira, C., Fontayne, A., Fowler-Jaeger, N., Clerici, C., Hummler, E., Rossier, B. C., and Planès, C. (2007) *J. Physiol.* **582**, 777–788
 34. Pradervand, S., Barker, P. M., Wang, Q., Ernst, S. A., Beermann, F., Grubb, B. R., Burnier, M., Schmidt, A., Bindels, R. J., Gatzky, J. T., Rossier, B. C., and Hummler, E. (1999) *Proc. Natl. Acad. Sci. U.S.A.* **96**, 1732–1737
 35. Snouwaert, J. N., Brigman, K. K., Latour, A. M., Malouf, N. N., Boucher, R. C., Smithies, O., and Koller, B. H. (1992) *Science* **257**, 1083–1088
 36. Grubb, B. R., Vick, R. N., and Boucher, R. C. (1994) *Am. J. Physiol.* **266**, C1478–C1483
 37. Grubb, B. R., Paradiso, A. M., and Boucher, R. C. (1994) *Am. J. Physiol.* **267**, C293–C300
 38. Dempster, J. (1993) *Computer Analysis of Electrophysiological Signals*, Academic Press, London
 39. Tarran, R., Button, B., Picher, M., Paradiso, A. M., Ribeiro, C. M., Lazrowski, E. R., Zhang, L., Collins, P. L., Pickles, R. J., Fredberg, J. J., and Boucher, R. C. (2005) *J. Biol. Chem.* **280**, 35751–35759
 40. Grubb, B. R., and Boucher, R. C. (1999) *Physiol. Rev.* **79**, S193–S214
 41. Tarran, R., Trout, L., Donaldson, S. H., and Boucher, R. C. (2006) *J. Gen. Physiol.* **127**, 591–604
 42. García-Añoveros, J., Ma, C., and Chalfie, M. (1995) *Curr. Biol.* **5**, 441–448
 43. Syntichaki, P., and Tavernarakis, N. (2002) *EMBO Rep.* **3**, 604–609
 44. Fyfe, G. K., and Canessa, C. M. (1998) *J. Gen. Physiol.* **112**, 423–432
 45. McNicholas, C. M., and Canessa, C. M. (1997) *J. Gen. Physiol.* **109**, 681–692
 46. Helms, M. N., Self, J., Bao, H. F., Job, L. C., Jain, L., and Eaton, D. C. (2006) *Am. J. Physiol. Lung Cell Mol. Physiol.* **291**, L610–L618
 47. Caldwell, R. A., Boucher, R. C., and Stutts, M. J. (2005) *Am. J. Physiol. Lung Cell Mol. Physiol.* **288**, L813–L819
 48. Diakov, A., Bera, K., Mokrushina, M., Krueger, B., and Korbmacher, C. (2008) *J. Physiol.* **586**, 4587–4608
 49. Kleyman, T. R., Carattino, M. D., and Hughey, R. P. (2009) *J. Biol. Chem.* **284**, 20447–20451
 50. Knowles, M. R., and Boucher, R. C. (2002) *J. Clin. Invest.* **109**, 571–577
 51. Mall, M. A. (2008) *J. Aerosol Med. Pulm. Drug Deliv.* **21**, 13–24
 52. Hopf, A., Schreiber, R., Mall, M., Greger, R., and Kunzelmann, K. (1999) *J. Biol. Chem.* **274**, 13894–13899
 53. Ji, H. L., Chalfant, M. L., Jovov, B., Lockhart, J. P., Parker, S. B., Fuller, C. M., Stanton, B. A., and Benos, D. J. (2000) *J. Biol. Chem.* **275**, 27947–27956
 54. Firsov, D., Schild, L., Gautschi, I., Méritat, A. M., Schneeberger, E., and Rossier, B. C. (1996) *Proc. Natl. Acad. Sci. U.S.A.* **93**, 15370–15375
 55. Mall, M., Kreda, S. M., Mengos, A., Jensen, T. J., Hirtz, S., Seydewitz, H. H., Yankaskas, J., Kunzelmann, K., Riordan, J. R., and Boucher, R. C. (2004) *Gastroenterology* **126**, 32–41
 56. Kreda, S. M., Mall, M., Mengos, A., Rochelle, L., Yankaskas, J., Riordan, J. R., and Boucher, R. C. (2005) *Mol. Biol. Cell* **16**, 2154–2167
 57. Vallet, V., Chraïbi, A., Gaeggeler, H. P., Horisberger, J. D., and Rossier, B. C. (1997) *Nature* **389**, 607–610
 58. Donaldson, S. H., Hirsh, A., Li, D. C., Holloway, G., Chao, J., Boucher, R. C., and Gabriel, S. E. (2002) *J. Biol. Chem.* **277**, 8338–8345
 59. Myerburg, M. M., Butterworth, M. B., McKenna, E. E., Peters, K. W., Frizzell, R. A., Kleyman, T. R., and Pilewski, J. M. (2006) *J. Biol. Chem.* **281**, 27942–27949
 60. Garcia-Caballero, A., Rasmussen, J. E., Gaillard, E., Watson, M. J., Olsen, J. C., Donaldson, S. H., Stutts, M. J., and Tarran, R. (2009) *Proc. Natl. Acad. Sci. U.S.A.* **106**, 11412–11417
 61. Zhou, Z., Treis, D., Schubert, S. C., Harm, M., Schatterny, J., Hirtz, S., Duerr, J., Boucher, R. C., and Mall, M. A. (2008) *Am. J. Respir. Crit. Care Med.* **178**, 1245–1256
 62. Hirn, C., Shapovalov, G., Petermann, O., Roulet, E., and Ruegg, U. T. (2008) *J. Gen. Physiol.* **132**, 199–208
 63. Perl, A. K., Tichelaar, J. W., and Whitsett, J. A. (2002) *Transgenic Res.* **11**, 21–29
 64. Livraghi, A., Mall, M., Paradiso, A. M., Boucher, R. C., and Ribeiro, C. M. (2008) *Am. J. Respir. Cell Mol. Biol.* **38**, 423–434
 65. Willumsen, N. J., Davis, C. W., and Boucher, R. C. (1989) *Am. J. Physiol.* **256**, C1033–C1044